P6.7

HIGH RESOLUTION NUMERICAL SIMULATIONS OF THUNDERSTORM OUTFLOW BOUNDARIES

Bruce D. Lee and Catherine A. Finley

Department of Earth Sciences - Meteorology
University of Northern Colorado, Greeley, Colorado

1. INTRODUCTION

Thunderstorm outflows represent a vehicle for potentially damaging surface winds and dangerous wind shear that impacts the aviation community. Yet, high resolution, three-dimensional numerical modeling studies adequate to resolve the fine-scale (~200-400 m) instabilities and their kinematic structures along outflows have not been done. Only recently, have comprehensive plans been implemented for observational study of boundaries at the necessary resolution to document the *fine-scale* three-dimensional structures (e.g., IHOP). Of particular interest is lobe and cleft instability (LCI, Simpson 1969, 1972) located in the gravitationally unstable region near the outflow nose where less-dense air is overrun by the outflow. Although a dominant instability type along outflows, LCI has received very little attention in the atmospheric sciences community likely due to the observational and computational restrictions associated with studying phenomenon on this scale.

Owing to past computational restrictions, most outflow simulations have been relegated to the two-dimensional vertical plane. In this configuration, adequate grid spacing was present to resolve Kelvin Helmholtz Instability (KHI) and analyze the kinematic two-dimensional fields (e.g., Droegemeier and Wilhelmson 1987). More recently, a few higher resolution (50-100 m horizontal grid spacing) three-dimensional numerical studies of outflow boundaries and related phenomena have been documented in the literature (e.g., Lee and Wilhelmson 1997a,b; Orf and Anderson 1999; Rao et al. 1999).

While the observational literature is rich in documentation of KHI, there are very few references to observed lobe and cleft instability. Mueller and Carbone's (1987) dual-Doppler study of a Colorado outflow revealed, along with other instabilities (KHI and horizontal shearing instability), a possible pattern of superimposed LCI at the outflow leading edge. Intrieri et al. (1990) employed Doppler lidar to identify lobe and cleft structure on the leading edge of a Colorado outflow boundary. Interestingly, Intrieri et al. suggested the possibility that the lobe and cleft structure might influence convection initiation in both single and colliding outflow scenarios. Ohno and Suzuki (1993) identified small high wind cores of a few hundred meters in length along the leading edge of the sea breeze front that were suggestive of LCI.

Our objective in this study is to gain a better understanding of the three-dimensional instabilities indigenous to the region at and within several kilometers of the outflow leading edge. This understanding is likely critical for explaining, at least in part, the damage pattern for outflow-associated severe wind events, the magnitude of both vertical and horizontal shears of importance to aviation, the development of gustnadoes, and possibly even the localized distribution of moist convective forcing along outflow boundaries.

Corresponding author address: Dr. Bruce D. Lee
Department of Earth Sciences - Meteorology
Univ. of Northern Colorado, Greeley, CO 80639
email: bdlee@.unco.edu

2. EXPERIMENT DESIGN

Simulations have be conducted using the MSTFLOW three-dimensional, nonhydrostatic, quasi-compressible, finite difference, convective cloud model (Lee and Wilhelmson 1997b). To adequately resolve outflow instabilities as small as LCI (typical length scale of several hundred meters), horizontal grid spacing of 40 m and a stretched vertical grid (40 m spacing at level 1) are utilized over a 21.6 x 4.0 x 7.2 km domain (540 x 100 x 60 grid). Boundary conditions are periodic in the north-south direction and open in the west-east direction. A semi-slip surface boundary condition is used. Since moist microphysics are not required for these simulations, all moist processes in the model have been turned off. The outflow boundary is created in the model via a quasi "dam break" initialization whereby a cold reservoir is allowed to collapse creating a density current in the model domain, similar to the technique employed in Lee and Wilhelmson (1997 a,b) and Klemp et al. (1994). The maximum θ deficit in this reservoir is -7.0 ^{o}K, a value representative of a strong summer outflow boundary (Mahoney 1988). The ambient environment is calm and statically neutral with θ = 300 ^{o}K through the depth of the domain. Results shown here are from the baseline simulation. The comprehensive suite of simulations will include parameter tests investigating the sensitivity of instability morphology to changes in cold pool strength, surface drag, and horizontal shear at the outflow leading edge. The latter of these tests should reveal the relationship between LCI instability and horizontal shearing instability (revealed observationally by gustnado locations). Results from some of these sensitivity tests will be shown at the conference.

3. RESULTS

The simulations have yielded a well-resolved pattern of KHI and LCI. The other dominant outflow leading edge instability type, horizontal shearing instability, would not be expected without a marked vertical vortex sheet at the leading edge (Lee and Wilhelmson 1997a). Figure 1 shows combination isosurface and volume renderings from 1800 and 3480

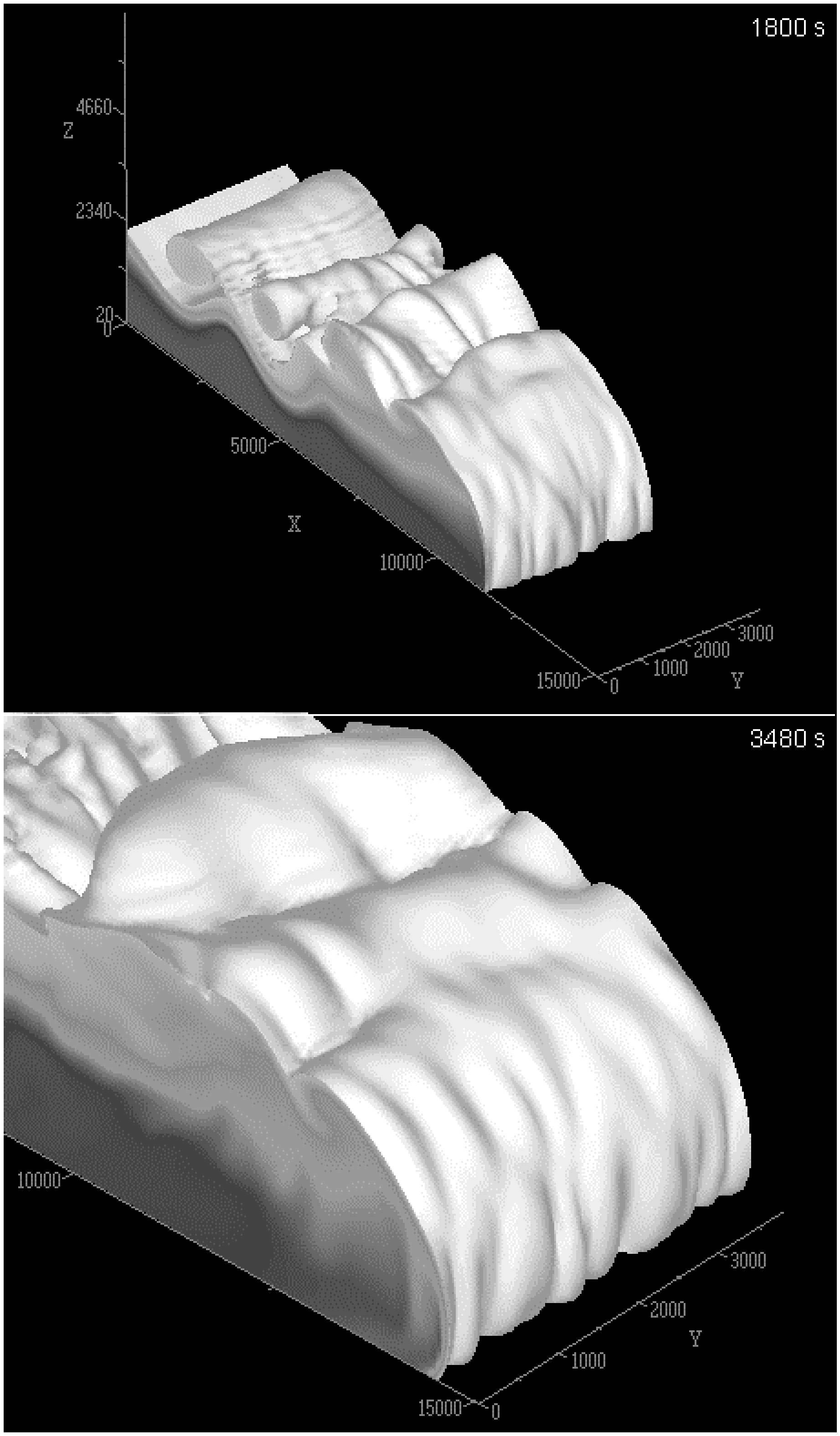

Fig. 1. Isosurface and volume renderings of the simulated outflow at 1800 and 3480 s. The gray scaled isosurface represents θ' of -1.5 ^{o}K. The XZ gray scaling shows the internal outflow temperature with darker shadings being colder. Note that the darkest shade represents a θ' of -7 ^{o}K. Only a 15 km long subset of the domain is used in these renderings.

s of the 3600 s simulation. Most numerical outflow simulations in the literature have been run with a "free-slip" lower boundary condition and lack a nose. In this run, the outflow's nose (seen best at 3480 s in Fig. 1) typically extended approximately 100 m in front of the surface thermal boundary and 100 - 150 m above the surface. These chararcteristics compare favorably with Goff's (1977) benchmark tower studies of outflows and Simpson's (1997) analysis of laboratory and atmospheric gravity current nose height data. It is the presence of this nose that allows for LCI development. As shown in Fig. 1, a vigorous LCI response is underway at the outflow leading edge. The figure looks reminiscent of pictures of haboob phenomena and laboratory density current experiments (Simpson 1997). The other obvious instability seen in Fig. 1 is the presence of KHI atop the boundary. The KHI develop vigorously in the shear zone near the elevated outflow head. As one would expect in a real atmospheric scenario, the LCI impose three-dimensionality on the KHI waves as can be seen in the images. This three-dimensional structure becomes far more prominent as the KHI waves propagate rearward relative to the leading edge. Preliminary analysis indicates that large KHI waves are associated with localized regions of high surface wind. Mahoney (1988) hypothesized that strong "microburst-like" surface wind patterns just behind an observed outflow leading edge could be due to large KHI waves extending to near the surface. The two-dimensional outflow simulations of Droegemeier and Wilhelmson (1987) also support the idea of KHI waves protruding well into the outflow body behind the head region. The divergent "microbrust-like" surface wind patterns in these observational cases wound not be caused by merely two-dimensional KHI, but rather, a highly three-dimensional flow feature (e.g., KHI that has been subject to tilting). Our simulations do show an increasingly non-linear pattern in the post-head region surface wind maxima after the KHI waves take on more three-dimensionality. Further analysis is required to ascertain the flow field and forcing mechanisms related to these trailing wind maxima.

An appreciation for the morphology of outflow LCI may be gained by comparing leading edge temperature structure at various times in the simulation as shown in Fig. 2. The lobe and cleft structure is continually evolving. As a lobe reaches some critical length, a new cleft bisects it forming 2 lobes where one previously existed. Clefts gradually close forming larger lobes, that then eventually attain this critical length. This process continues until the outflow has weakened to the point where a nose cannot be sustained. In this simulation, the number of lobes ranged from 6 to 12 with an average number of 9.7. There was no tendency for the average lobe length to increase or decrease through the 3600 s simulation. Average lobe size was about 400 m. Had the simulation been run with smaller grid spacing, this number would likely be somewhat higher, but is not too far from the predicted average lobe size of 325 m based on a 1.3 km head height (Simpson 1997).

Given the short time scale nature of LCI evolution, the kinematic aspects of the flow field such as vorticity couplets, horizontal shear zones, local updraft perturbations, and wind maximums are constantly changing. For instance, an aircraft encountering the outflow leading edge at a particular line-relative geographical location at some given time would likely realize markedly different conditions on a second pass through the same location just 5 min. later. Figure 3 shows select low-level model fields at 1920 s to illustrate anomalies associated with the LCI. Lobes are regions of wind maxima with the highest winds located in regions where the lobe structure is undergoing rapid evolution such as the lobe/cleft transition areas between y = 2 - 3 km. We hypothesize that in outflows significantly more intense than this one, these evolving lobes could be regions of initial damaging winds. The marked wind gradients shown (horizontal shear zones) correspond to transient but intense vertical vorticity zones that usually are organized in couplets aligned with each cleft. As shown in the figure, the positive and negative vorticity centers are often of asymmetric intensity but vigorous ($\zeta \sim 0.1\ s^{-1}$). One other facet of the leading edge clefts involves their role in controlling the distribution of vertical velocity. Narrow, low-level updraft jet-like maxima exist in the clefts. At just 100 m AGL, updraft speeds

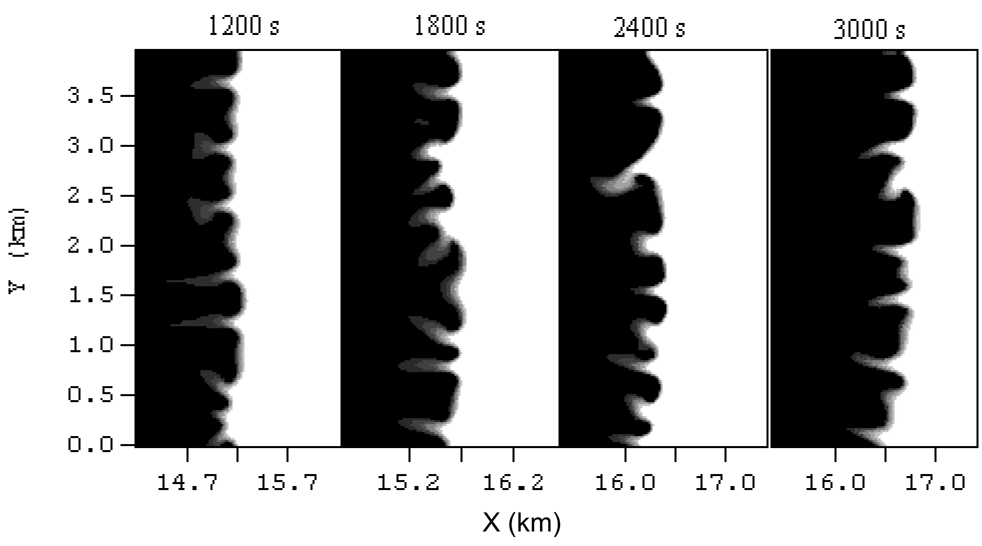

Fig. 2. XY plots of the leading edge θ' field at the surface for a 2 km section of the domain.

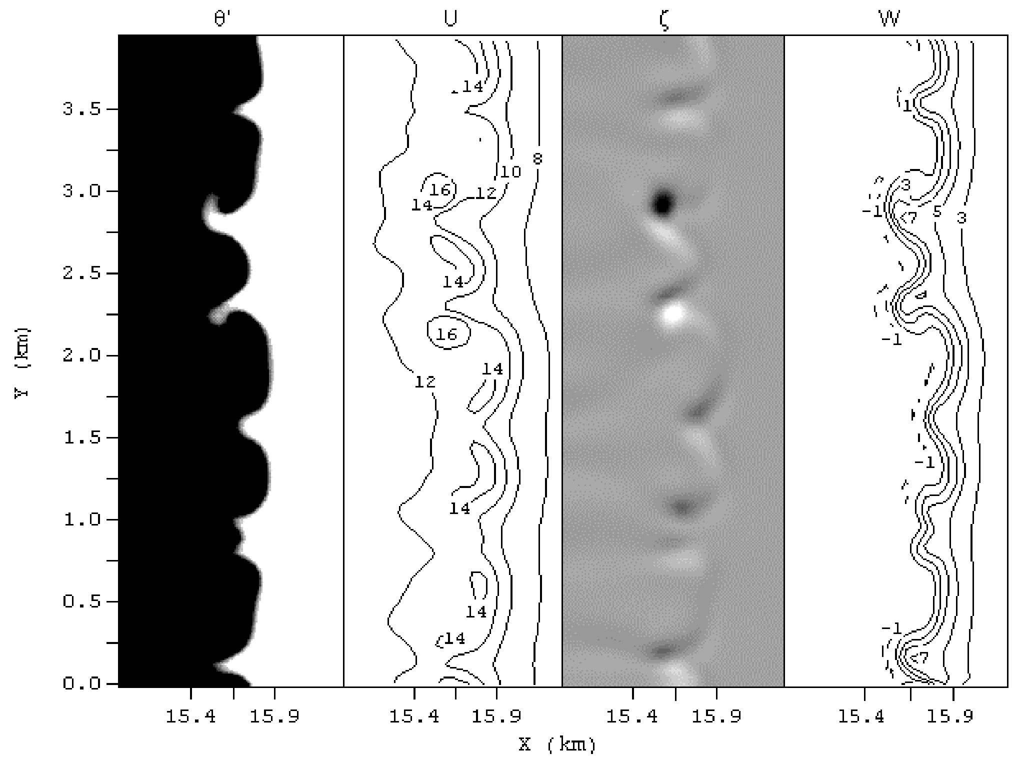

Fig. 3. θ', u, vertical vorticity and w fields at 1920 s. All fields are at the surface except w, which is at 240 m. For perspective, the vertical vorticity grayscale ranges from negative values of approx. -0.1 s^{-1} (darkest shading) to positive values of approx. 0.1 s^{-1} (lightest shading).

approach 5 m s^{-1} and are nearly 8 m s^{-1} at 240 m. These updraft structures are as transient as their parent cleft structures. The narrow updraft jets represent another LCI leading edge anomaly that could be hazardous to aviation. Whether or not these cleft updraft jets have a role in moist convective forcing remains a question for ongoing analysis.

3. CONCLUSIONS

The results presented here clearly identify potential regions of instability-related wind maxima at and near the leading edge of outflows that could represent initial areas of damaging winds. The analysis additionally indicates high wind shear regions from LCI, beyond those normally associated with KHI, that likely are significant aviation hazards. Results will be presented at the conference of 25-30 m grid point simulations of the baseline case as well as other parameter experiments noted in the introduction. Please note that a companion paper (P2.4), employing radar data analysis from a severe Colorado outflow, provides some rare observational documentation of LCI.

4. ACKNOWLEDGEMENTS

This research was supported by the National Science Foundation under grant ATM-0105279.

5. REFERENCES

Droegemeier, K. K., and R. B. Wilhelmson, 1987: Numerical simulation of thunderstorm outflow dynamics. Part I: Outflow sensitivity experiments and turbulence dynamics. *J. Atmos. Sci.*, **44,** 1180-1210.

Goff, R. C., 1976: Vertical structure of thunderstorm outflows. *Mon. Wea. Rev.*, **104**, 1429-1440.

Intrieri, J. M., A. J. Bedard, Jr., and R. M. Hardesty, 1990: Details of colliding thunderstorm outflows as observed by Doppler lidar. *J. Atmos. Sci.*, **47**, 1081-1098.

Klemp, J. B., R. Rotunno, and W. C. Skamarock, 1994: On the dynamics of gravity currents in channel. *J. Fluid Mech.,* **269**, 169-198.

Lee, B. D., and R. B. Wilhelmson, 1997b: The numerical simulation of non-supercell tornadogenesis. Part II: Evolution of a family of tornadoes along a weak outflow boundary. *J. Atmos. Sci.*, **54**, 2387-2415.

Lee, B. D., and R. B. Wilhelmson, 1997a: The numerical simulation of non-supercell tornadogenesis. Part I: Initiation and evolution of pre-tornadic misocyclone circulations along a dry outflow boundary. *J. Atmos. Sci.,* **54**, 32-60.

Mahoney, W. P., 1988: Gustfront characteristics and the kinematics associated with interacting thunderstorm outflows. *Mon. Wea. Rev.,* **116,** 1474-1491.

Mueller, C. K., and R. E. Carbone, 1987: Dynamics of a thunderstorm outflow. *J. Atmos. Sci.,* **15,** 1879-1898.

Ohno, H., and O. Suzuki, 1993: Small-scale high wind cores enhancing low-level wind shear: Doppler radar observations of opposing wind adjacent to the sea-breeze frontal zone on 10 September 1989. *Meteorol. Atmos. Phys*. **52**, 147-152.

Orf, L., G., and J. R. Anderson (1999): A numerical study of traveling microbursts. *Mon. Wea. Rev.*, **127**, 1244-1257.

Rao, P. A., H. E. Fuelberg, and K. K. Droegemeier, 1999: High-resolution modeling of the Cape Canaveral area land-water circulations and associated features. *Mon. Wea. Rev.,* **127**, 1808-1821.

Simpson, J. E., 1969: A comparison between laboratory and atmospheric density currents. *Q. J. R. Meteorol. Soc.,* **95**, 758-765.

Simpson, J. E., 1972: Effects of the lower boundary on the head of a gravity current. J. Fluid Mech., 53, 759-768.

Simpson, J. E., 1997: *Gravity Currents. In the Environment and Laboratory*. Second Ed., Cambridge Univ. Press, Cambridge, England, 244 pp.